Quadrature Formulas, the Complex Plane, Fractional Derivatives, and Underground Sensing

Bengt Fornberg

University of Colorado, Boulder
Department of Applied Mathematics

Quadrature Formulas: Some very classical methods

Trapezoidal rule: Fit by piecewise linear functions (Babylonian astronomers, 50 BC)

Gives weights $h\left[\frac{1}{2}\ 1\ \ 1\ \ 1\ \ 1\ \ 1\ \ldots\ 1\ \frac{1}{2}\right]$

Simpson's rule: Fit by succession of quadratics

Simpson (1710-1761); however used by Kepler (1571-1630) ▶▶▶▶

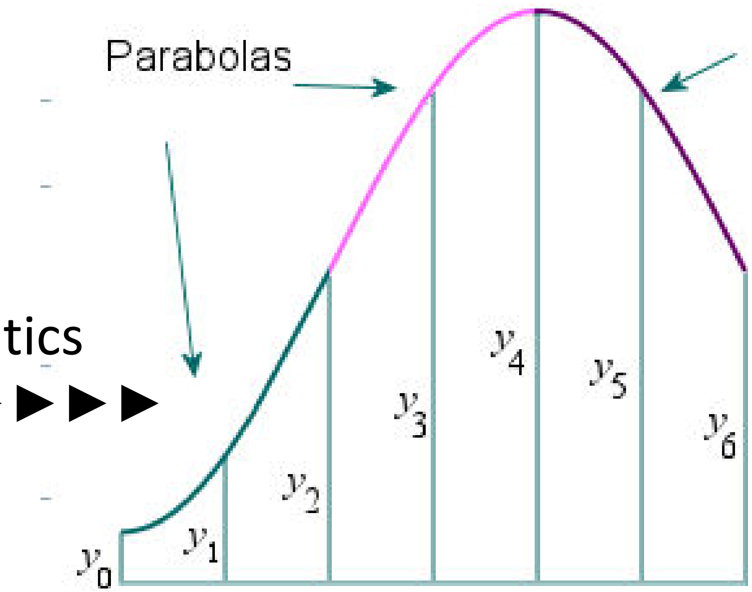

Gives weights $\frac{h}{3}\left[1\ \ 4\ \ 2\ \ 4\ \ 2\ \ 4\ \ 2\ldots\ 4\ \ 1\right]$

Newton-Cotes: Continue the Simpson's rule concept by using piecewise cubics, quartics, etc. Newton (1642-1726), Cotes (1682-1716)

Newton-Cotes concept is flawed for several reasons:

- Virtually all errors in the Trapezoidal Rule comes from the ends of the interval – one should do corrections there and NOT damage the accuracy throughout the interior.
- For periodic problem, Simpson gives only half the number of correct digits compared to the Trapezoidal rule.
- Newton-Cotes becomes very unstable for increasing orders.

Gregory's method: James Gregory (1638-1675)

Adjust weighs at the interval ends before all weights become one throughout the interior of the interval

$p =$									
2	$\frac{1}{2}$								
3	$\frac{5}{12}$	$\frac{13}{12}$							
4	$\frac{3}{8}$	$\frac{7}{6}$	$\frac{23}{24}$						
5	$\frac{251}{720}$	$\frac{299}{240}$	$\frac{211}{240}$	$\frac{739}{720}$					
6	$\frac{95}{288}$	$\frac{317}{240}$	$\frac{23}{30}$	$\frac{739}{720}$	$\frac{157}{160}$				
7	$\frac{19087}{60480}$	$\frac{84199}{60480}$	$\frac{18869}{30240}$	$\frac{37621}{30240}$	$\frac{55031}{60480}$	$\frac{61343}{60480}$			
8	$\frac{5257}{17280}$	$\frac{22081}{15120}$	$\frac{54851}{120960}$	$\frac{103}{70}$	$\frac{89437}{120960}$	$\frac{16367}{15120}$	$\frac{23917}{24192}$		
9	$\frac{1070017}{3628800}$	$\frac{5537111}{3628800}$	$\frac{103613}{403200}$	$\frac{261115}{145152}$	$\frac{298951}{725760}$	$\frac{515677}{403200}$	$\frac{3349879}{3628800}$	$\frac{3662753}{3628800}$	
10	$\frac{25713}{89600}$	$\frac{1153247}{725760}$	$\frac{130583}{3628800}$	$\frac{903527}{403200}$	$-\frac{797}{5670}$	$\frac{6244961}{3628800}$	$\frac{56621}{80640}$	$\frac{3891877}{3628800}$	$\frac{1028617}{1036800}$
$\vdots$	$\vdots$	$\vdots$	$\vdots$	$\vdots$	$\vdots$	$\vdots$	$\vdots$	$\vdots$	$\vdots$ $\ddots$

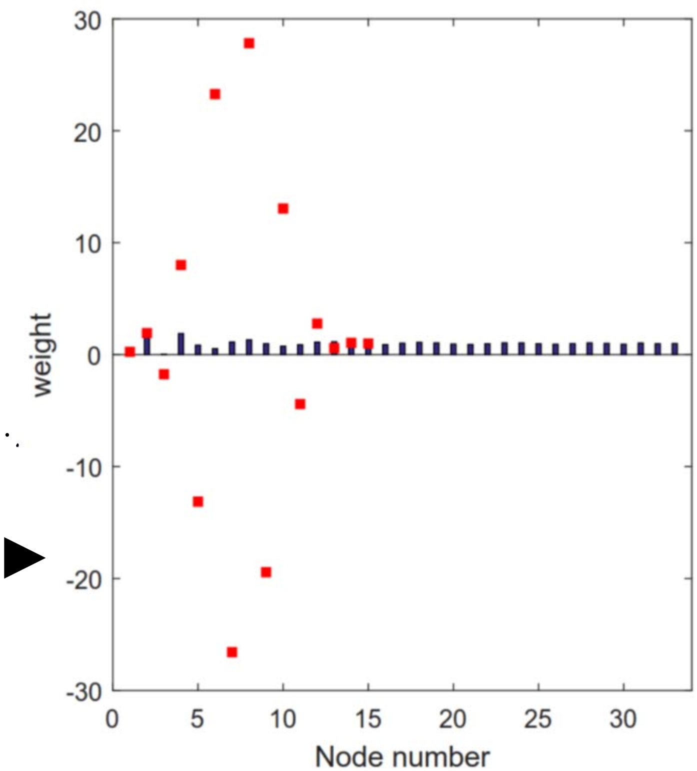

Collaboration with Jonah Reeger

Weights for the $O(h^{16})$ Gregory scheme (red) vs. for a wider scheme (black) of same order (now with all weights positive)

Enhanced end correction method applied to a test function

Test function: $f(x) = \cos(20\sqrt{x})$

$$\int_0^1 f(x)dx = \frac{1}{200}(\cos(20) + 20\sin(20) - 1)$$

Test function with *N* = 68; gives error < 10 $^{-14}$

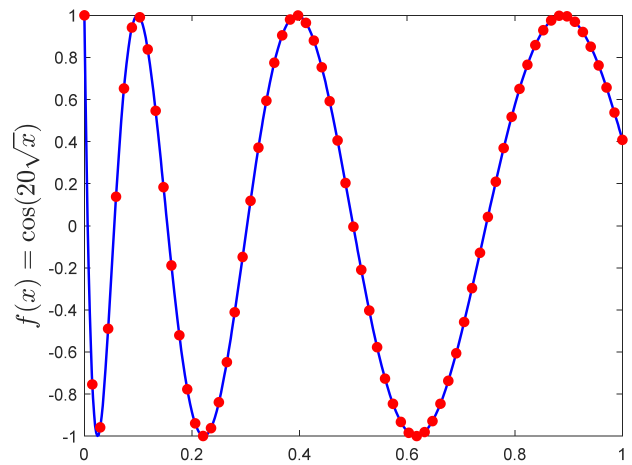

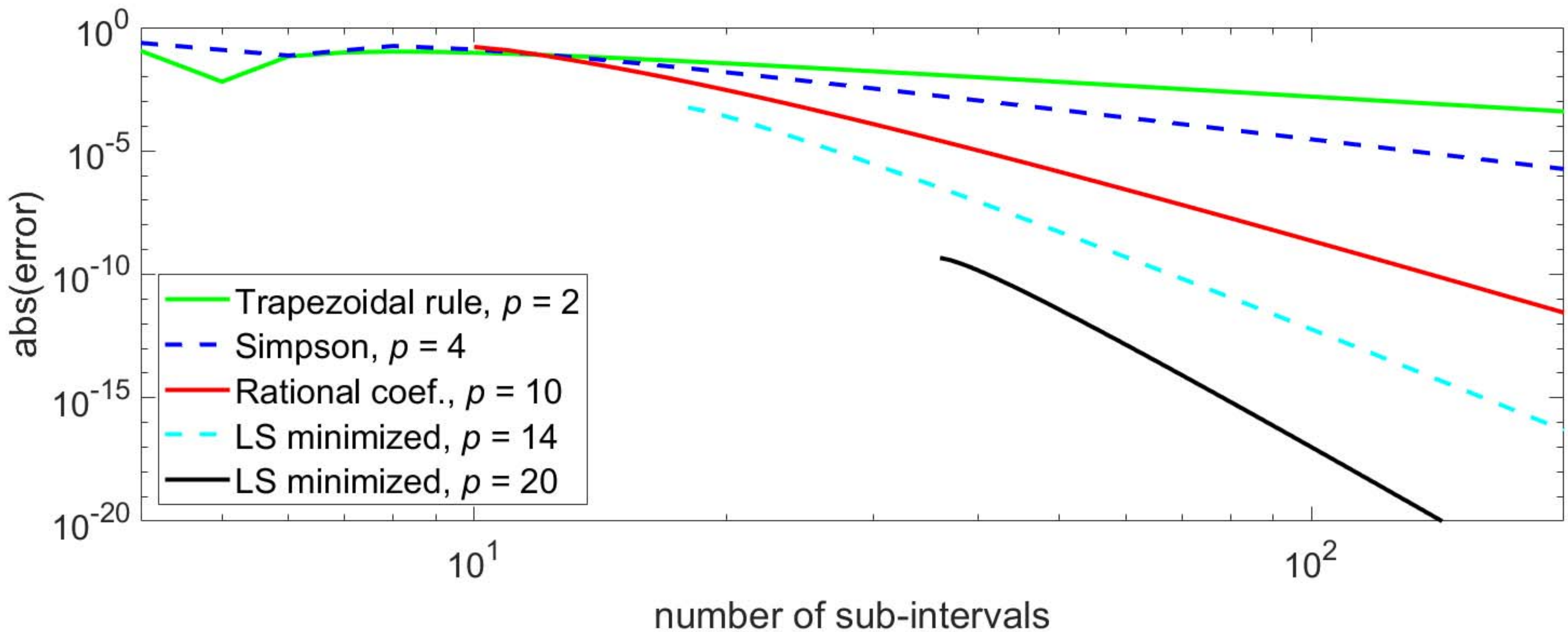

Some finite difference (FD) background

A few historical notes

c 1592 Jost Bürgi (interpolation in trigonometric tables)

17th century Calculus (limit of FD approximations)

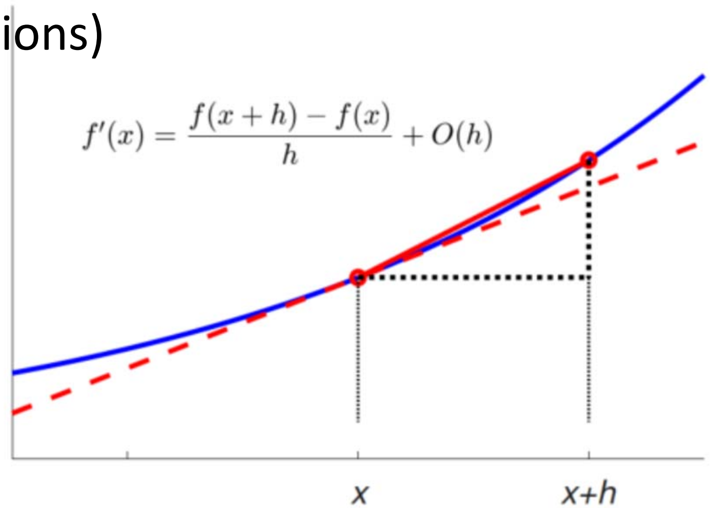

19th century Numerical ODE solvers developed and applied to finance and astronomy

20th century Numerical PDE solvers (Richardson, 1911)
Led to FEM, FVM, PS methods.

First derivative

order	weights								
2				$-\frac{1}{2}$	0	$\frac{1}{2}$			
4			$\frac{1}{12}$	$-\frac{2}{3}$	0	$\frac{2}{3}$	$-\frac{1}{12}$		
6		$-\frac{1}{60}$	$\frac{3}{20}$	$-\frac{3}{4}$	0	$\frac{3}{4}$	$-\frac{3}{20}$	$\frac{1}{60}$	
8	$\frac{1}{280}$	$-\frac{4}{105}$	$\frac{1}{5}$	$-\frac{4}{5}$	0	$\frac{4}{5}$	$-\frac{1}{5}$	$\frac{4}{105}$	$-\frac{1}{280}$
	↓	↓	↓	↓	↓	↓	↓	↓	↓
PS limit	$\frac{1}{4}$	$-\frac{1}{3}$	$\frac{1}{2}$	-1	0	1	$-\frac{1}{2}$	$\frac{1}{3}$	$-\frac{1}{4}$

Second derivative

order	weights								
2				1	-2	1			
4			$-\frac{1}{12}$	$\frac{4}{3}$	$-\frac{5}{2}$	$\frac{4}{3}$	$-\frac{1}{12}$		
6		$\frac{1}{90}$	$-\frac{3}{20}$	$\frac{3}{2}$	$-\frac{49}{18}$	$\frac{3}{2}$	$-\frac{3}{20}$	$\frac{1}{90}$	
8	$-\frac{1}{560}$	$\frac{8}{315}$	$-\frac{1}{5}$	$\frac{8}{5}$	$-\frac{205}{72}$	$\frac{8}{5}$	$-\frac{1}{5}$	$\frac{8}{315}$	$-\frac{1}{560}$
	↓	↓	↓	↓	↓	↓	↓	↓	↓
PS limit	$-\frac{2}{4^2}$	$\frac{2}{3^3}$	$-\frac{2}{2^2}$	$\frac{2}{1^2}$	$-\frac{\pi^2}{3}$	$\frac{2}{1^2}$	$-\frac{2}{2^2}$	$\frac{2}{3^3}$	$-\frac{2}{4^2}$

Complex Plane: FD formulas

Analytic functions form a very important special case of general 2-D functions $f(x,y)$.

Definition: With $z = x + iy$ complex, $f(z)$ is *analytic* if

$$\frac{\mathrm{d}f}{\mathrm{d}z} = \lim_{\Delta z \to 0} \frac{f(z+\Delta z) - f(z)}{\Delta z}$$

is uniquely defined, no matter from which direction Δz approaches zero.

Virtually all standard and special functions of applied sciences generalize for complex arguments to analytic functions.

Some consequences of analyticity:

FD formulas in the complex x,y-plane, applied to analytic functions, are vastly more efficient / accurate than classical FD formulas.

- No distinction between $\dfrac{\partial f}{\partial x}$ and $\dfrac{\partial f}{\partial y}$;
- Cauchy's integral formula: $f^{(k)}(z_0) = \dfrac{k!}{2\pi i} \oint_\Gamma \dfrac{f(z)}{(z-z_0)^{k+1}} dz$, $k = 0, 1, 2, \ldots$

A few examples of complex plane FD formulas

$$f'(0) = \frac{1}{40h}\begin{bmatrix} -1-i & -8i & 1-i \\ -8 & 0 & 8 \\ -1+i & 8i & 1+i \end{bmatrix} f + O(h^8),$$

$$f''(0) = \frac{1}{20h^2}\begin{bmatrix} i & -8 & -i \\ 8 & 0 & 8 \\ -i & -8 & i \end{bmatrix} f + O(h^8),$$

......

$$f^{(4)}(0) = \frac{3}{10h^4}\begin{bmatrix} -1 & 16 & -1 \\ 16 & -60 & 16 \\ -1 & 16 & -1 \end{bmatrix} f + O(h^8),$$

......

$$f^{(8)}(0) = \frac{504}{h^8}\begin{bmatrix} 1 & 4 & 1 \\ 4 & -20 & 4 \\ 1 & 4 & 1 \end{bmatrix} f + O(h^4),$$

$$f'(0) = \frac{1}{h}\begin{bmatrix} \frac{1+i}{477360} & \frac{4(-1-i)}{29835} & \frac{i}{1326} & \frac{4(1-i)}{29835} & \frac{-1+i}{477360} \\ \frac{4(-1-i)}{29835} & \frac{8(-1-i)}{351} & \frac{-8i}{39} & \frac{8(1-i)}{351} & \frac{4(1-i)}{29835} \\ \frac{1}{1326} & -\frac{8}{39} & 0 & \frac{8}{39} & -\frac{1}{1326} \\ \frac{4(-1+i)}{29835} & \frac{8(-1+i)}{351} & \frac{8i}{39} & \frac{8(1+i)}{351} & \frac{4(1+i)}{29835} \\ \frac{1-i}{477360} & \frac{4(-1+i)}{29835} & \frac{-i}{1326} & \frac{4(1+i)}{29835} & \frac{-1-i}{477360} \end{bmatrix} f + O(h^{24})$$

Extremely high accuracies already for very small stencils

The weights at location μ + iν, with μ,ν integers, decay to zero like $O(e^{-\frac{\pi}{2}(\mu^2+\nu^2)})$

As the accuracy order is increased (or goes to the PS limit), approximations remain local.

Combine equispaced quadrature with analytic functions:

The Euler-Maclaurin formula

(1740 – 70 years after Gregory)

$$\int_{x_0}^{\infty} f(x)dx = h\sum_{k=0}^{\infty} f(x_k) - \frac{h}{2} f(x_0) + \frac{h^2}{12} f^{(1)}(x_0) - \frac{h^4}{720} f^{(3)}(x_0) + \frac{h^6}{30240} f^{(5)}(x_0) - \frac{h^8}{1209600} f^{(7)}(x_0) + - \ldots$$

Recall trapezoidal rule (TR) approximation:

$$\int_0^{\infty} f(x)dx = h\left\{\frac{1}{2} \quad 1 \quad 1 \quad 1 \quad 1 \quad 1 \quad 1 \quad \ldots\right\} f + O(h^2)$$

With 3x3 stencils, one can approximate odd derivatives up through $f^{(7)}(0)$. Doing this gives

$$\int_0^{\infty} f(x)dx = h\left\{\begin{bmatrix} \frac{-821-779i}{403200} & -\frac{1889i}{100800} & \frac{821-779i}{403200} \\ -\frac{1511}{100800} & \left\{\frac{1}{2}\right. & 1+\frac{1511}{100800} \\ \frac{-821+779i}{403200} & \frac{1889i}{100800} & \frac{821+779i}{403200} \end{bmatrix} \quad 1 \quad 1 \quad 1 \quad 1 \quad 1 \quad \ldots \right\} f + O(h^{10})$$

- Magnitude of weights in 5x5 stencil case ▶▶▶▶
  Correction weights very small compared to TR weights.

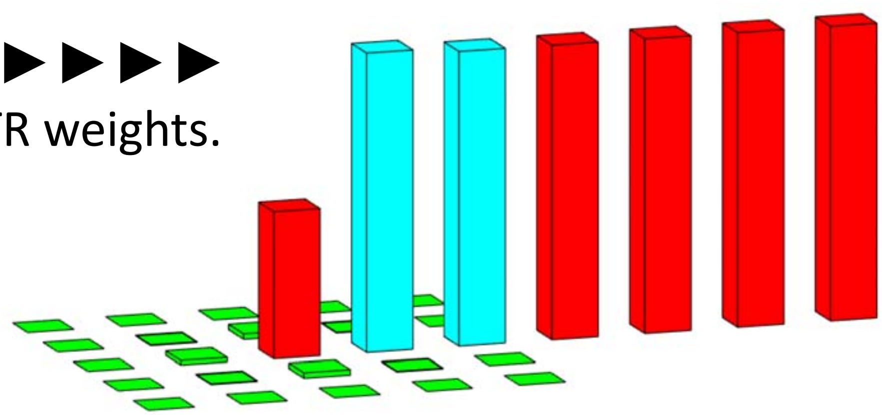

- Accuracy order one above the number of stencil points (in figure $O(h^{26})$)

- For finite interval, matching expansion at the opposite end

Numerically approximate contour integrals in the complex plane

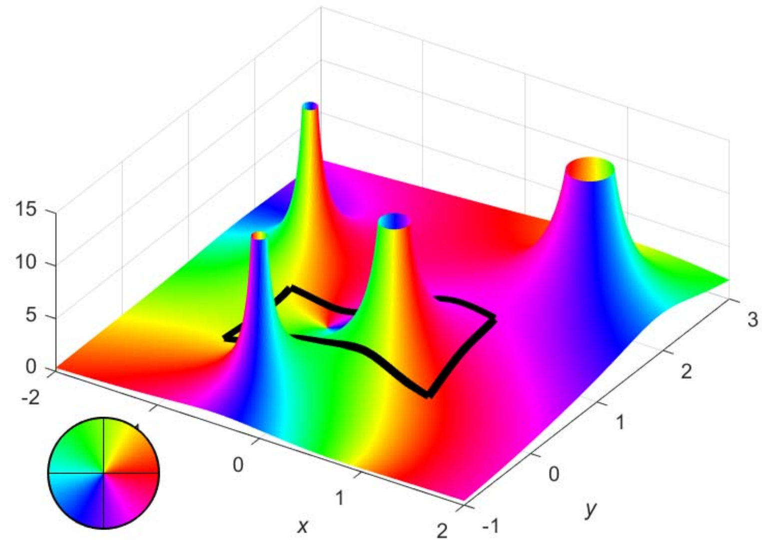

Magnitude and phase angle

Test function illustrated:

$$f(z)=\frac{2}{z-0.4(1+i)}-\frac{1}{z+0.4(1+i)}+\frac{1}{z+1.2-1.6i}-\frac{3}{z-1.3-2i}$$

Contours can be open or closed

We want to only use grid point values
(no other functional information)

Using 7x7 'correction stencils' at each path corner gives accuracy ordrer $O(h^{50})$.
Grid density shown sufficient for error around 10^{-40}

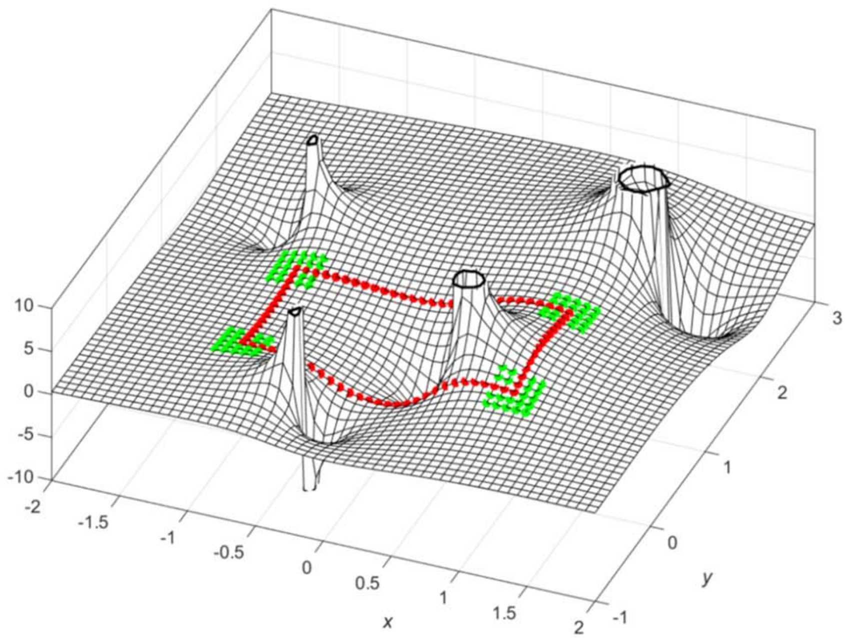

Real part

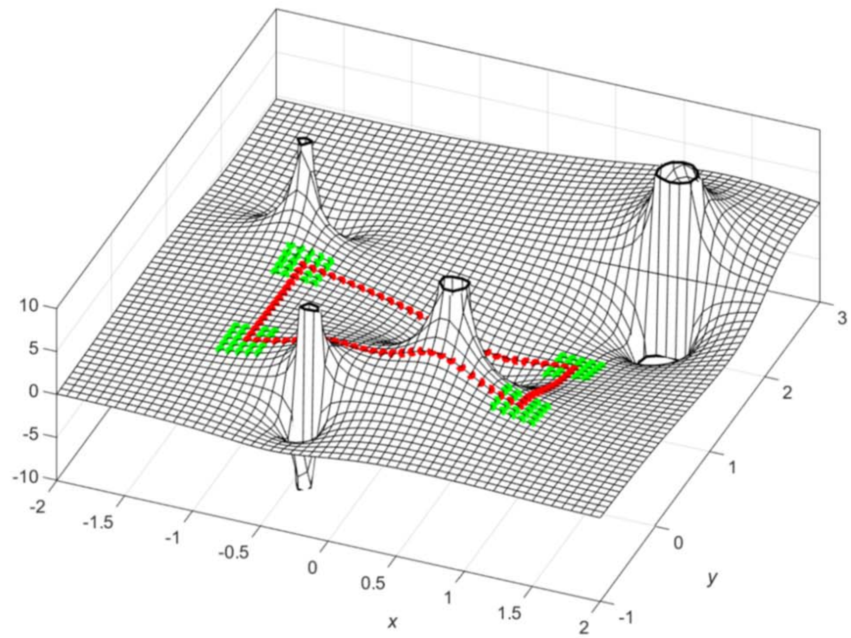

Imaginary part

Fractional derivatives:

Origin of Fractional derivatives

1695 l'Hôpital asked Leibnitz about derivatives of order ½ to which Leibniz replied
"This is an apparent paradox from which one day, useful consequences will be drawn"

1823 Abel presented a complete framework for fractional calculus, and a first application

From 1832 Major further contributions by Liouville, Riemann, etc.

There are many ways to define fractional derivatives. It was recently (2022) discovered that all main versions belong to a two-parameter family.

Two most commonly used types of fractional derivatives

Riemann-Liouville (1832, 1847):

$$ {}_0^{RL}D_t^{\alpha} f(t) = \frac{1}{\Gamma(n-\alpha)} \frac{d^n}{dt^n} \int_0^t \frac{f(\tau)}{(t-\tau)^{\alpha+1-n}} d\tau, \qquad n-1 < \alpha < n $$

- For m integer $D^{\alpha+m}f(t) = D^m D^\alpha f(t)$
- Limit $\alpha \to$ integer is continuous

Caputo (1967):

$$ {}_0^{C}D_t^{\alpha} f(t) = \frac{1}{\Gamma(n-\alpha)} \int_0^t \frac{\frac{d^n}{d\tau^n} f(\tau)}{(t-\tau)^{\alpha+1-n}} d\tau, \qquad n-1 < \alpha < n $$

- For m integer $D^{\alpha+m}f(t) = D^\alpha D^m f(t)$
- D(constant) = 0
- Solving fractional ODEs requires easy initial conditions ICs

Note also:

Fractional derivatives (as defined above) typically singular at $t = 0$.

Fractional erivatives of e^t

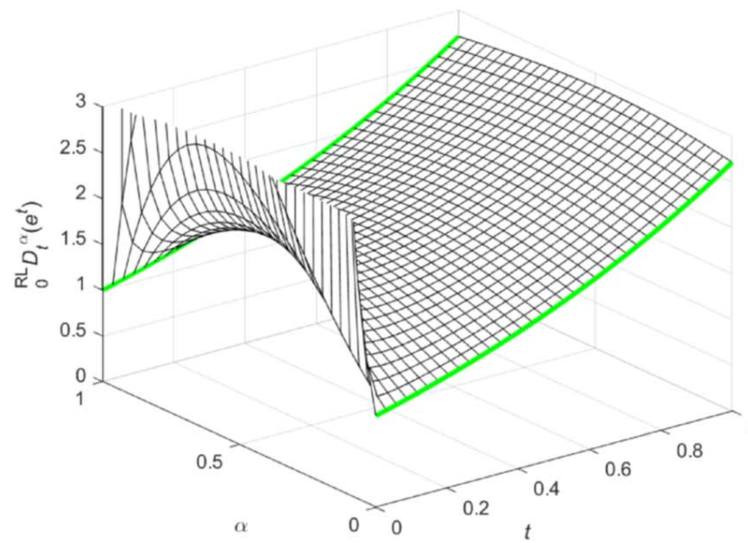

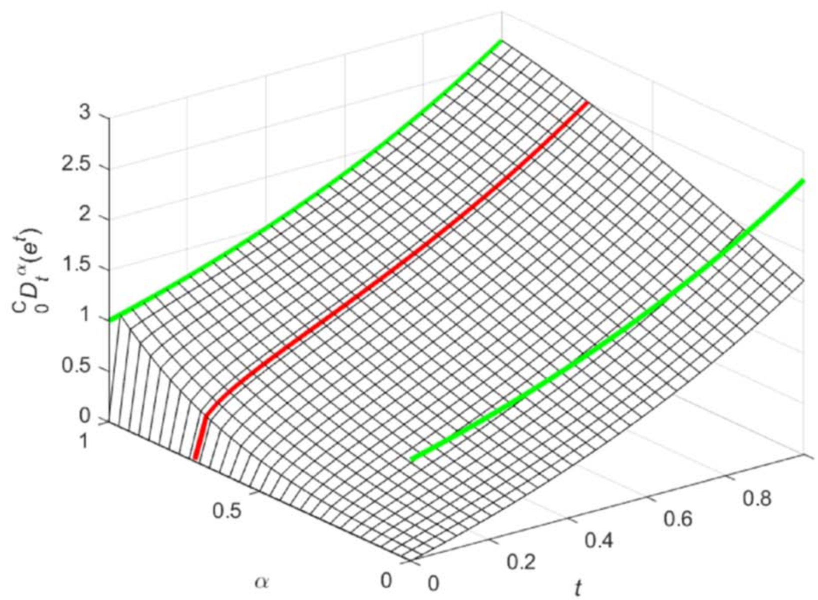

Recall the Caputo derivative:

$$D^{\alpha} f(z) = \frac{1}{\Gamma(1-\alpha)} \int_0^z \frac{f'(\tau)}{(z-\tau)^{\alpha}} d\tau, \qquad 0<\alpha<1$$

Theorem: If $f(z)$ is analytic, so is $D^{\alpha} f(z)$ (typically with branch point at $z = 0$).

Preliminary step for numerics: Integrate by parts once, to get $f(\tau)$ instead of $f'(\tau)$.

Key novel result:

Collaboration with Cécile Piret, Caleb Jacobs, Andrew Lwrence and Austin Higgins.

The integral end correction methods just described generalize immediately to the singular integral that arises for fractional derivatives.

Vast amount of other applications of fractional derivatives

- Fractional diffusion

  Recall heat / diffusion equation $u_t = u_{xx}$.

  i. Fractional in time, $D^{\alpha}{}_{t}\, u = u_{xx}$ with $\alpha \approx 1$, provides 'memory'

  ii. Fractional in space, $u_t = D^{\alpha}{}_{x}\, u$ with $\alpha \approx 2$, often represents better various 'anomalous' diffusion processes (typically with 'base point' on each side).

- Frequency-dependent wave propagation
- Random walks
- Active damping of flexible structures
- Gas/solute transport/reactions in porous media
- Epidemiology (incl. asymptomatic spreading)
- Modeling of bone/tissue growth/healing
- Modeling of shape memory materials
- Economic processes with memory
- Modeling of supercapacitors / advanced batteries using nano-materials
- **Solving the 3-D Laplace equation as an initial value problem**

  Mathematically ill-posed, but central to mineral prospecting based on aerial gravity and magnetic measurements.

Two novel ways to continue aerial survey data downwards

Collaboration with Jeff Thurston

1. Fractional Laplacian

Gravity and magnetic potentials (and their gradients) satisfy the3-D Laplace equatuion $\left(\frac{\partial^2}{\partial x^2}+\frac{\partial^2}{\partial y^2}+\frac{\partial^2}{\partial z^2}\right)u=0$

Data is recorded on undulating surface (flown by airplane or helicopter)

1. Computationally transfer data to flat surface (RBF-based fractional derivative-based method – unpiublished)
2. Continue downward (knowing that *u* should decay upwards)

- Write the 3-D Laplace equation as $\frac{\partial^2 u}{\partial z^2}=-\left(\frac{\partial^2}{\partial x^2}+\frac{\partial^2}{\partial y^2}\right)u=(-\Delta)^1 u \;\Rightarrow\; \frac{\partial u}{\partial z}=(-\Delta)^{1/2}u=v$ (fractional 2-D Laplacian)
- Next, solve ODE system $\frac{d}{dz}\begin{pmatrix}u\\ v\end{pmatrix}=\begin{pmatrix}v\\ -\Delta u\end{pmatrix}$ towards negative *z.*

Left figure:

Magnetic recording, Central BC, Canada

Example of recorded surface z = 0 data

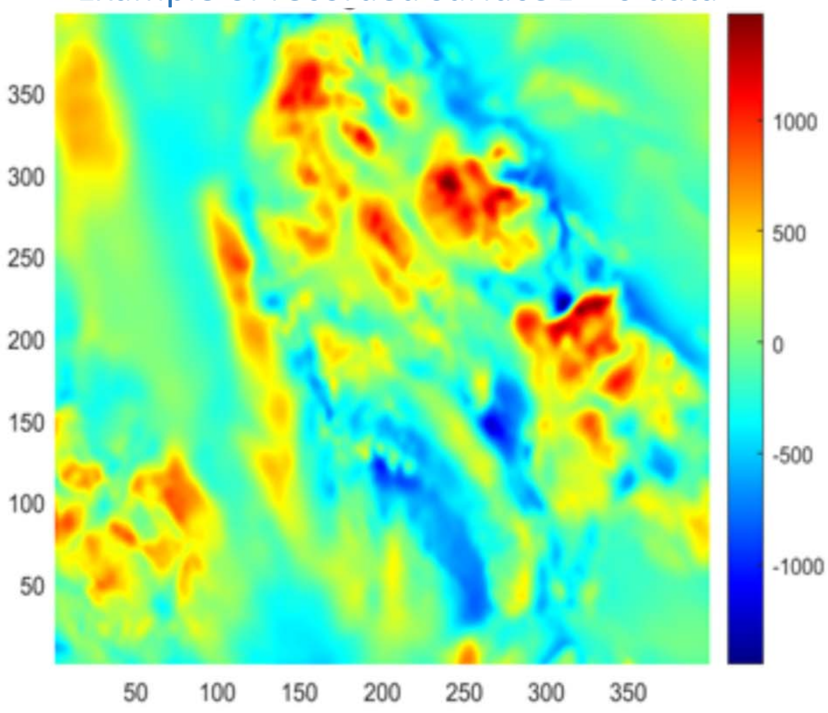

Contunied downwards to z = -100 meters as described

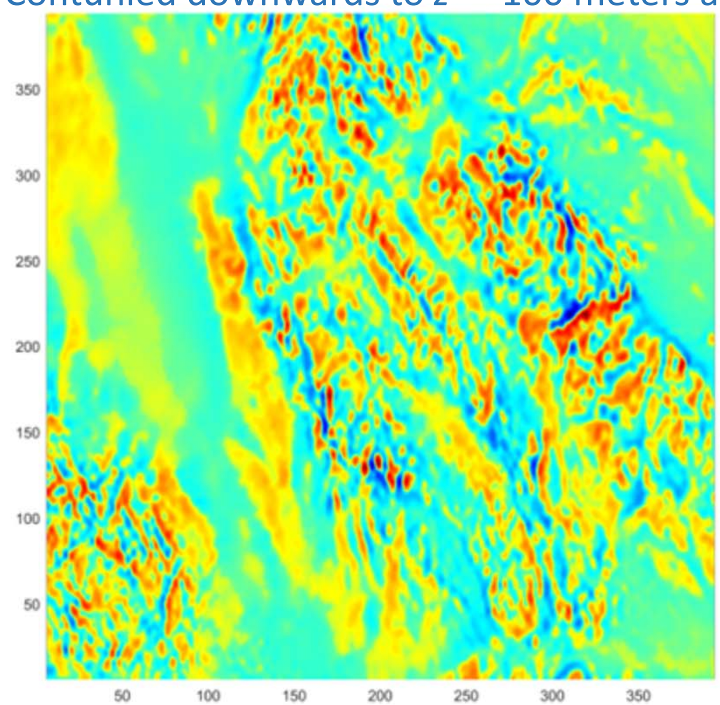

2. Padé continuation

An entirely different (also novel) approach to again extract seemingly non-present data from magnetic or gravity aerial survey recordings.

Mathematical background:

Given a truncated Taylor series $T_{m+n}(z) = \sum_{k=0}^{m+n} c_k z^k$ convert it to Padé rational form $P_n^m(z) = \dfrac{\sum_{k=0}^{m} a_k z^k}{\sum_{k=0}^{n} b_k z^k}$

Algorithm:

Put the two expressions equal, multiply up denominator and equate coefficients

Relatively straightforward to convert $\{c_k\}$ to $\{a_k, b_k\}$ and vice versa.

Mathematical Padé Example:

Given only a small number of leading Taylor coefficients for

$$f(z) = \frac{\log(1+z)}{z} = 1 - \frac{1}{2}z + \frac{1}{3}z^2 - \frac{1}{4}z^4 + \ldots$$

approximate *f*(2) (with analytical value $f(2) = \dfrac{\log 3}{2} \approx 0.549306144$).

Note: The evaluation point $z = 2$ is well outside the region of convergence $|z| < 1$ for the Taylor series.

Mathematical Padé example - continued

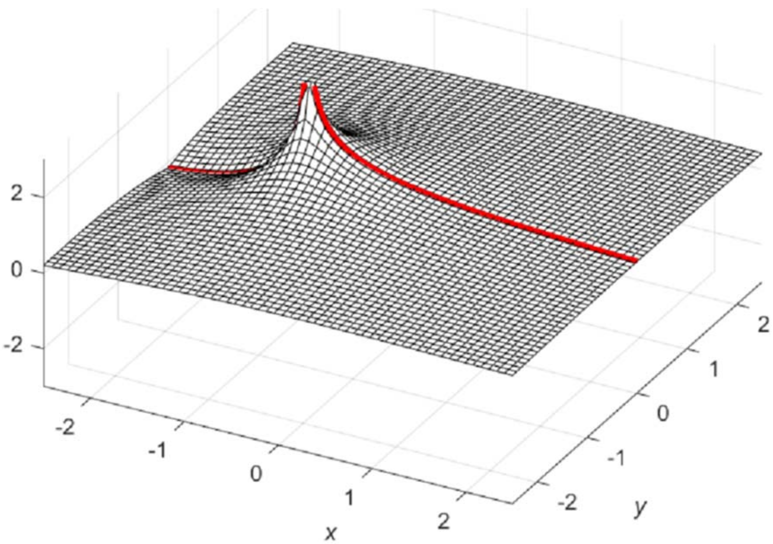

Real part of $f(z) = \dfrac{\log(1+z)}{z}$

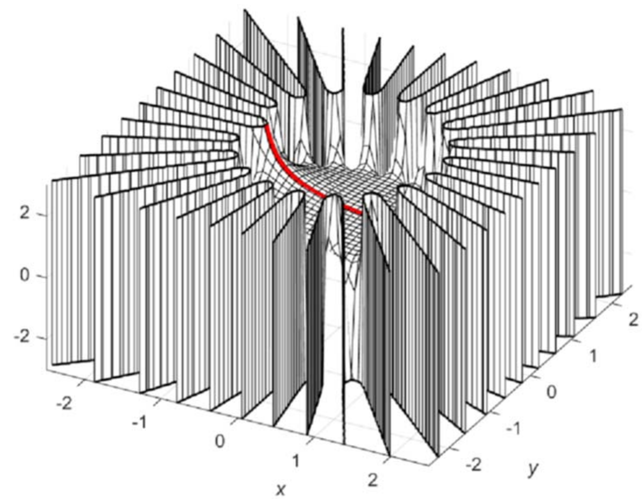

Real part of $T^{20}(z)$

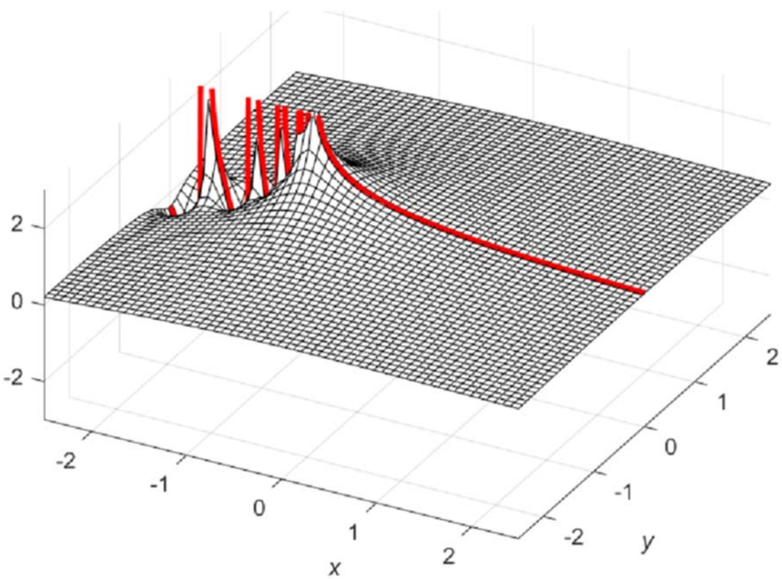

Real part of $P_{10}^{10}(z)$

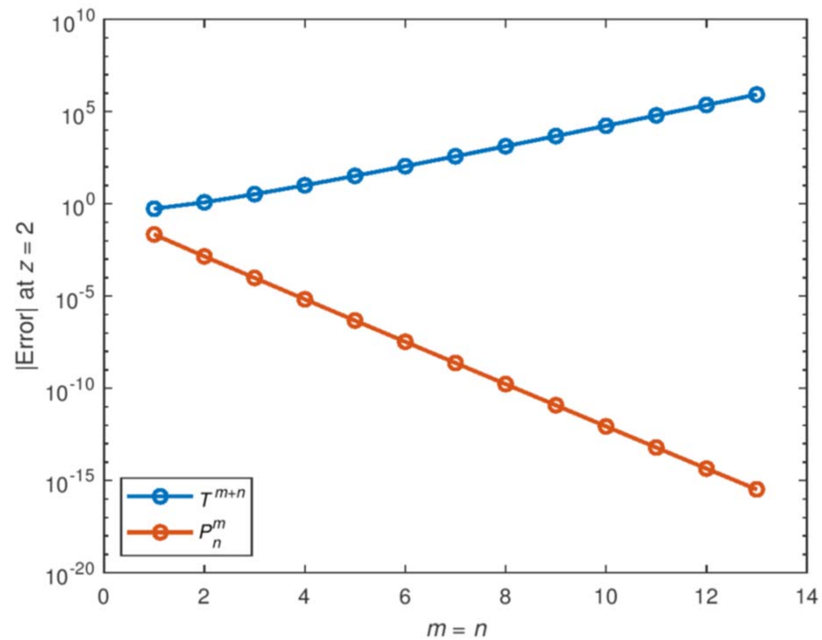

Error in $P_n^n(2)$ for m = n = 10 approximately 10^{-12}.

Downward continuation via Padé approximations

Make the line of data the *x*-axis in an imagined vertical complex *x*,*y*-plane.

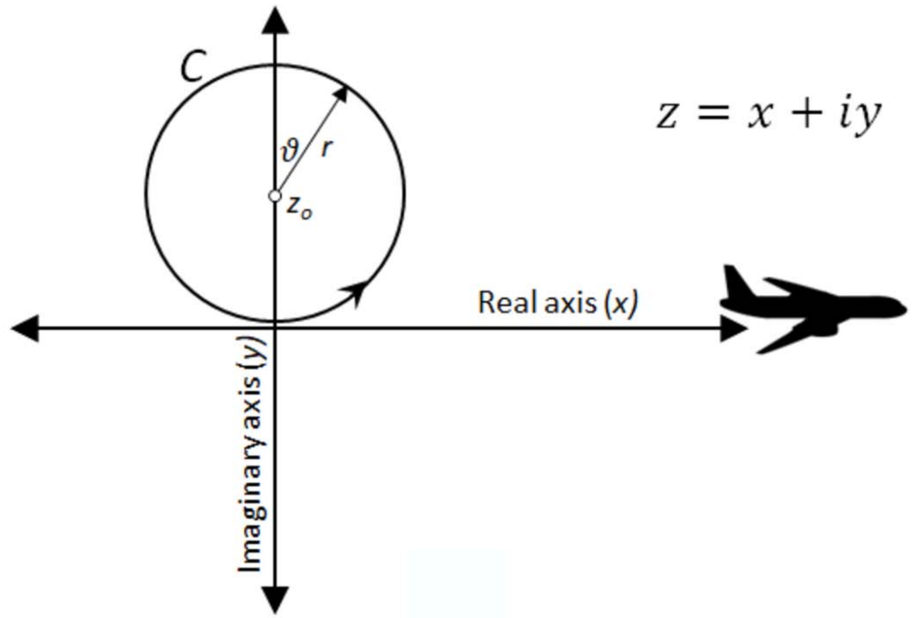

Perform a numerical Hilbert transform on the data. This gives an analytic function that satisfies the 2-D Laplace equation and decays upward.

Evaluate at sequence of elevations. By 1-D interpolation, get equispaced data around a circle. FFT gives Taylor coefficients, convert to Padé.
Evaluate this below ground.

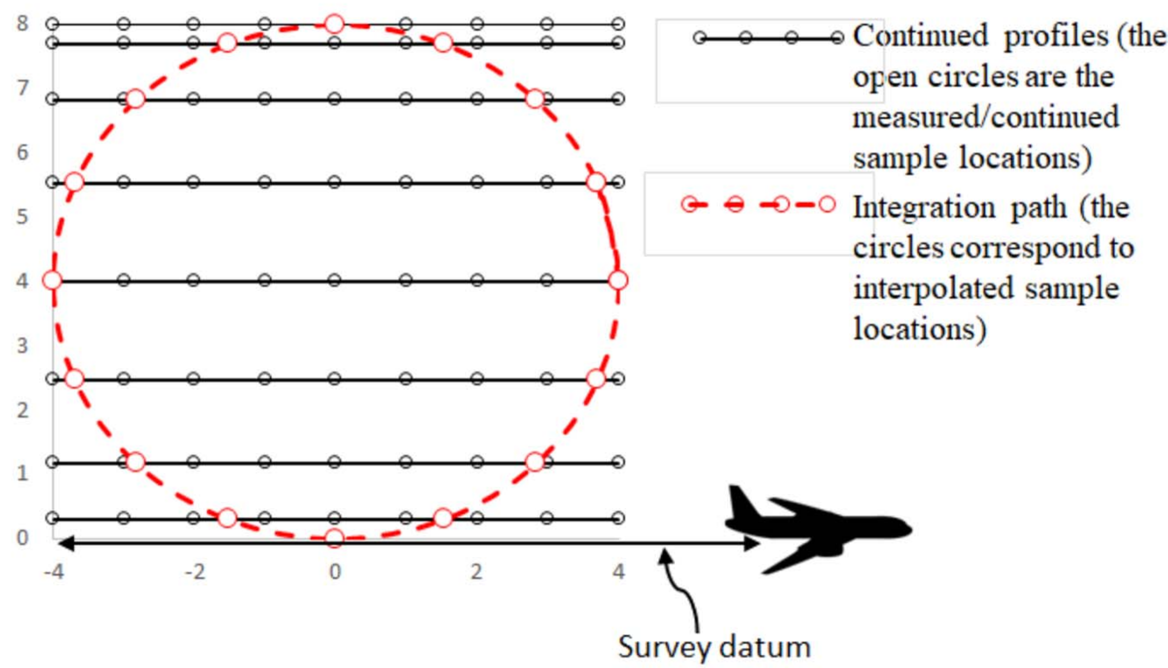

Padé continuation – Two examples of downward continuation

‘State-of-the-art’ continuation | Padé continuation

Gravity data, central BC, Canada

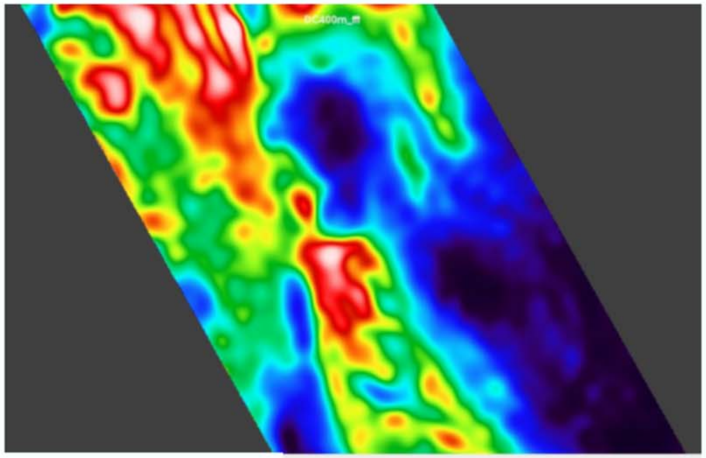

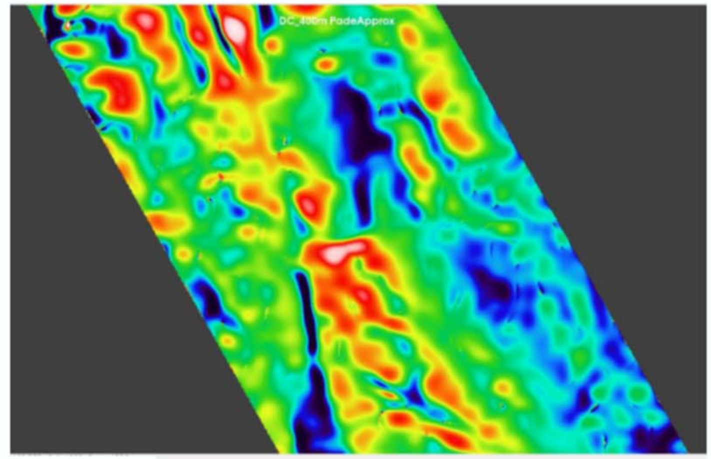

Gravity data, Victoria, Australia

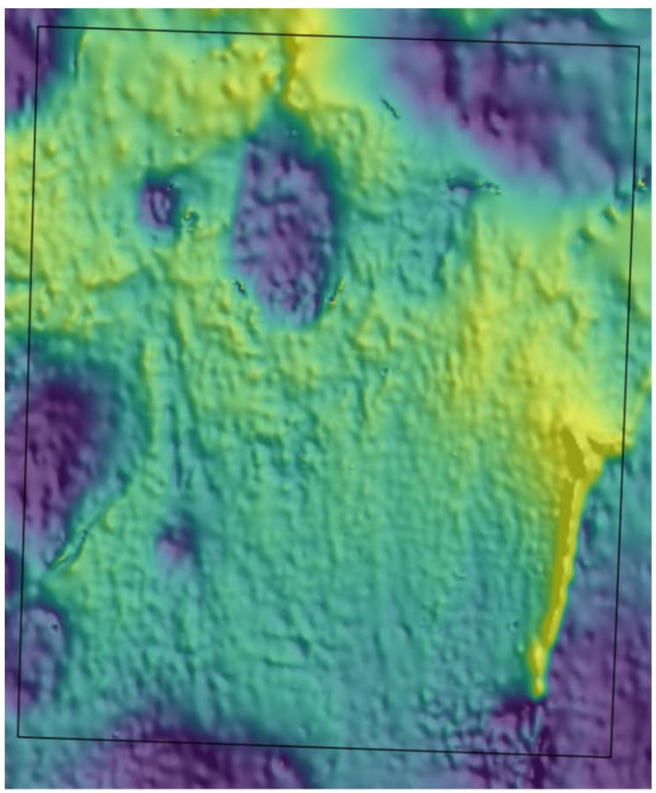

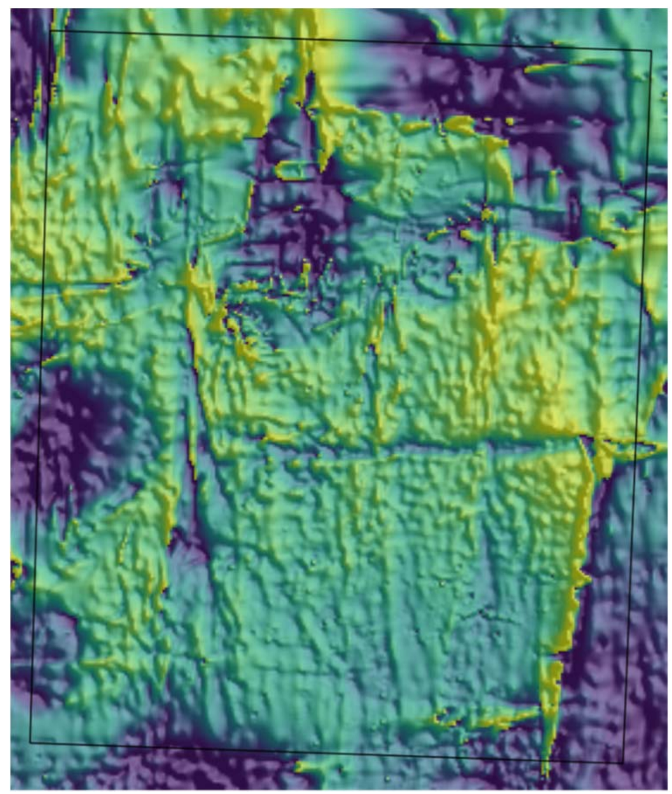

Figures to the right from FitzGerald, Thurston, Cottew, EAGE 2022.

Example of detecting underground voids - The SSC (Superconducting Super Collider)

LEB – Low energy booster

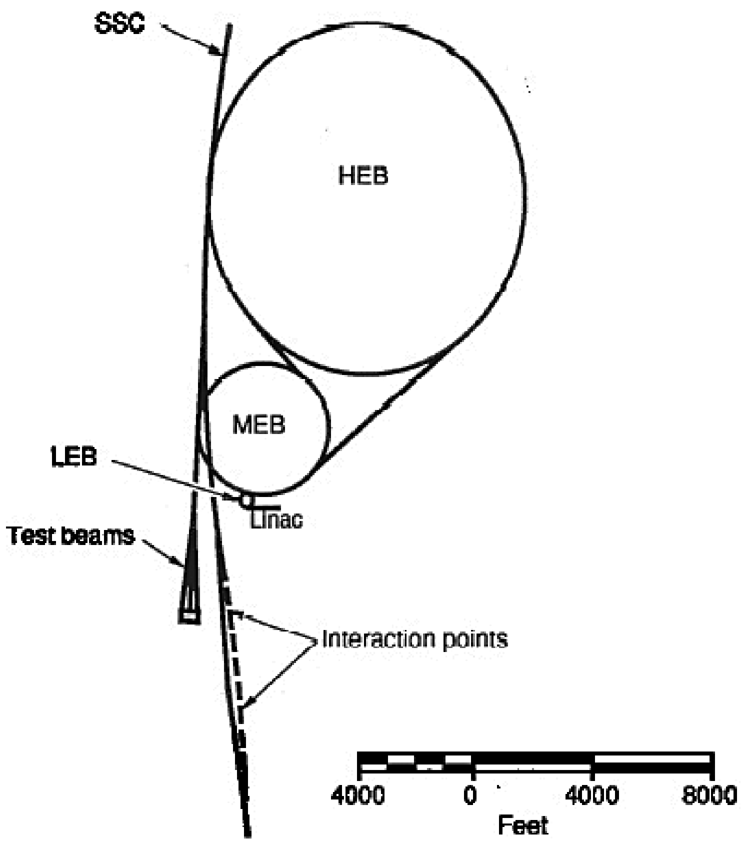

2010 'Falcon' aerial survey

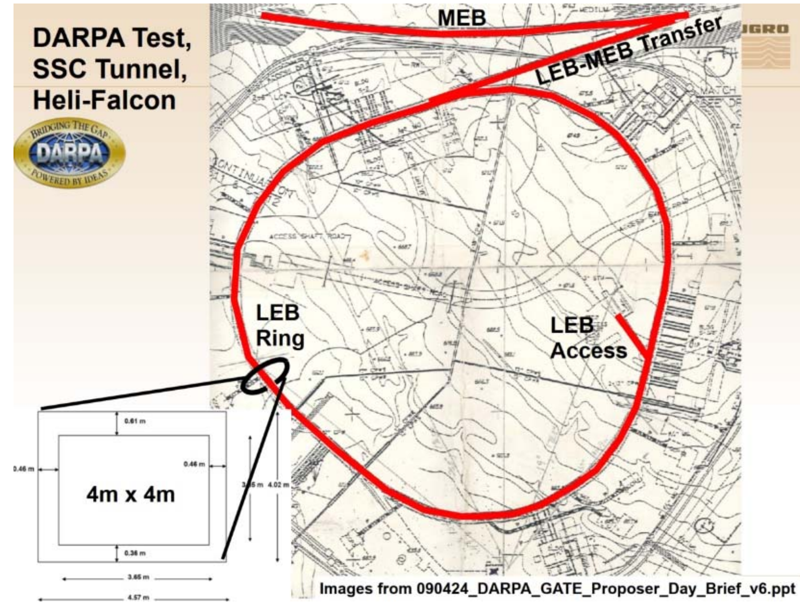

Images from 090424_DARPA_GATE_Proposer_Day_Brief_v6.ppt

Terrain-Corrected GDD, DARPA Test Survey

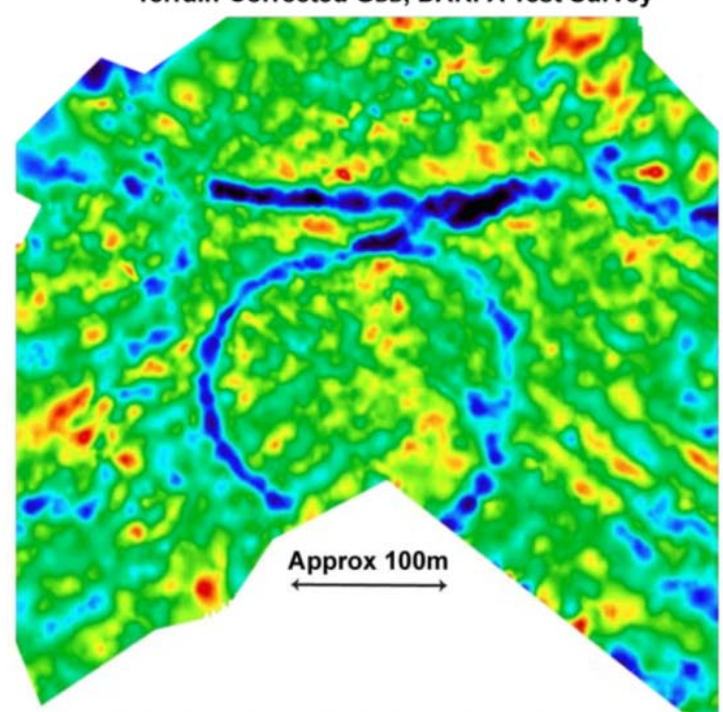

Figure 2: Falcon data collected over LEB ring of SSC: 4m tunnel at approx 5m depth.

Data from 090424_DARPA_GATE_Proposer_Day_Brief_v6.ppt

Some conclusions

Regular derivatives and integrals:

- Derivatives and Contour integrals of grid-based analytic functions can be evaluated to very high levels of accuracy already on coarse grids.

Fractional derivatives:

- Fractional derivatives of analytic functions can also be computed to machine precision accuracy using grids with density comparable to what is needed for typical functional displays.

Mineral prospecting:

Research on the topics above has led to two novel approaches for continuing aerial gravity and magnetic recordings downwards

- Fractional Laplacian together with finite differences (FD)
- Padé continuation

Some papers relevant to this presentation:

B.F. and J.A. Reeger, *An improved Gregory-like method for 1-D quadrature*, Numer. Math. 141 (2019), 1-19.
B.F., *Improving the accuracy of the trapezoidal rule*, SIAM Review 63 (2021), 167-180.
B.F., *Generalizing the trapezoidal rule in the complex plane*, Numerical Algorithms 87 (2021), 187-202.
B.F., *Finite difference formulas in the complex plane*, Numerical Algorithms 90 (2022), 1305-1326.
B.F. and C. Piret, *Computation of fractional derivatives of analytic functions*, J. of Sci. Comp, 96 (2023), No. 79.
J.B. Thurston and B.F., Analytic continuation: A tool for aeromagnetic data interpretation, The Leading Edge (2024), 154-160.

Two books relevant to this presentation:

B.F. and C. Piret, *Complex Variables and Analytic Functions: An Illustrated Introduction*, SIAM (2020).
B.F. *High Accuracy Finite Difference Methods*, Cambridge University Press (2024).